IET Generation, Transmission & Distribution

Research Article

IET Journals
The Institution of Engineering and Technology

Multi-verse optimisation: a novel method for solution of load frequency control problem in power system

ISSN 1751-8687
Received on 10th April 2017
Accepted on 11th June 2017
E-First on 7th August 2017
doi: 10.1049/iet-gtd.2017.0296
www.ietdl.org

Dipayan Guha[1] ✉, Provas Kumar Roy[2], Subrata Banerjee[3]

[1]*Department of Electrical Engineering, Dr. B.C. Roy Engineering College, Durgapur, West Bengal, India*
[2]*Department of Electrical Engineering, Kalyani Government Engineering College, Kalyani, West Bengal, India*
[3]*Department of Electrical Engineering, National Institute of Technology, Durgapur, West Bengal, India*
✉ *E-mail: guha.dipayan@yahoo.com*

Abstract: In this article, a maiden attempt has been made to derive an optimal and effective outcome of load frequency control problem (LFC) using a novel evolutionary algorithm called multi-verse optimisation. The main inspiration of this algorithm is based on three concepts in cosmology: white hole, black hole, and wormhole. To show the effectiveness, a four-area hydrothermal power plant with distinct proportional-integral-derivative (PID) controller is investigated at the first instant and then the study is forwarded to the five-area thermal power plant. To enhance the dynamic stability, an optimal PID plus double-derivative controller (PID + DD) is designed and included in the control areas. The superiority of the proposed method has been established over some recently addressed control algorithms by transient analysis method. To add some degree of non-linearity, generation rate constraint and governor dead band are included in the model and their impacts on the system dynamics have been examined. Finally, a random load perturbation is given to the test systems to affirm the robustness of the designed controllers.

1 Introduction

As the loading demand and complexity of the modern power system increases day by day, therefore, it is immense to control the system frequency to its pre-defined value in order to hold the synchronisation between the control areas and to provide secure, reliable, and stable power supply to the consumers. Since the term frequency is directly correlated with system loading, thus any abrupt change in the loading cause serious perturbation in system frequency from its tolerance value. An abnormal change in frequency even causes blackout of the power system. Hence, continuous monitoring of power generation and loading demand is needed, which is done by load frequency controller (LFC). It keeps the difference between generation and demand, called area control error (ACE), to zero or minimum. The LFC regulates the governor valves in order to control the flow of steam to the turbine so as to regulate the power generation. In today's scenario, LFC is one of the most important ancillary services in the power system. The LFC scheme is not only maintaining the frequency level, it offers a steady flow of power through tie-line between the nearby control areas. Whenever the system is experienced load perturbation, primary controller mainly served by the speed governing system match the generation with demand; however, the oscillations and steady-state errors persist in frequency and tie-line power which is nullified by the LFC. The important functions of LFC are enumerated below [1, 2].

(a) The steady-state frequency error due to step change in load must approach to zero as time progresses. As well as the transient frequency and time errors should be low.
(b) The tie-line power errors following a load perturbation in any control area should be zero provided each area carry its own load.
(c) Any area in need of power during any emergency should assist other areas.

Recently, LFC analysis has received a great attention from the researchers because of its usefulness in power system operation and control. Different control strategies have been employed in LFC area over the last few decades, although the majority of these studies are focused on the design of proportional-integral-derivative (PID) controllers or its variants. An extensive literature review on LFC problem is available in [3]. In [4], different types of conventional controllers are reported and compared so as to identify the best controller among them. However, this study was limited to thermal power system. In [5], authors have employed fuzzy logic-based integral-double-derivative controllers for the effective solution of LFC problem and established the superiority of the proposed scheme over others reported control algorithms. Though the controller based on fuzzy logic provide a substantial improvement in the system performance, but it suffers from large momentary oscillation in the transient response as well as no specific mathematical relationship is defined to decide the scaling factor, rule base, membership function for the FLC. Additionally, it takes too much time to decide the rules for the knowledge base processes and the number of rules will increase with the order of power system. The intelligent controllers based on artificial neural network (ANN), an adaptive neuro-fuzzy interface system (ANFIS) are proposed in [6]. However, these types of controllers require large training data set for the supervised learning, demands high computational cost, selecting the number of layers, and a number of neurons in the layers. Further, ANN requires on-line model identification, which is really a tuff job for the large power plant. Yousef [7] has described an adaptive fuzzy logic control strategy for LFC of a multi-area power system. Tripathy *et al.* [8, 9] have examined the effect of governor dead band (GDB) non-linearity on the system dynamics of an interconnected power system and the describing function method was used to identify the linear approximated model of same. Recently, Guha *et al.* [10] have proposed an optimal PID controller for a possible solution of LFC problem and show its supremacy over other existing control algorithms. Two degrees of freedom PID controllers are deployed in [11] and performances are compared with PI/PID controllers. The advantages of fractional order controller over integral order controller are established in [12]. Besides these, some investigation has been carried out using H_∞ controller [13], internal model controller [14], sliding mode controller [15], μ-synthesis controller [16] etc. and show a substantial improvement of the system performance. The difficulties associated with H_∞ controller is the selection of weighting factor and pole-zero cancellation associated with it produces unwanted oscillations. Additionally, the order of

H_∞ controller is more than that of plant and requires deep user skills. These give rise to complexity in the design and inapplicable to implement [17]. Recently, in [18], Raju *et al.* have employed PID plus double-derivative (PID + DD) controller for the possible solution of LFC problem. However, this study is limited to three-area thermal power plant only. Additionally, authors have only considered generation rate constraint (GRC) non-linearity to show its performance in LFC area. Thus to explore the acceptability of PID + DD controllers for the large non-linear interconnected power system, further investigation is required.

Owing to the time-varying nature of power system, the operating point is changed in every minute. Thus, the fixed value controllers designed at nominal operating condition is no longer able to provide satisfactory performance. To overcome the said problem, researchers proposed different types of meta-heuristic optimisation techniques for searching a near globally optimal solution. In [19], cuckoo search algorithm (CSA) has employed to tune the PI-controller gains for three-area thermal power plant. Differential evolution (DE) has very simple structure and can be effortlessly applied to LFC problem in [20]. Another most popular optimisation technique is genetic algorithm (GA) and applied to LFC analysis in [21]. However, the premature convergence of GA degrades its search ability. Farhangi *et al.* [22] have used emotional learning-based optimisation for optimal design of intelligent controllers. Some investigation have been reported on bacteria foraging optimisation algorithm (BFOA) [5], teaching–learning-based optimisation (TLBO) [11, 15], bat algorithm [17], antlion optimisation [18], backtracking search algorithm (BSA) [23], tabu search algorithm (TSA) [24], biogeography-based optimisation (BBO) [25]. In [26–28], authors have presented quasi-oppositional harmony search algorithm for LFC of power system. Sahu *et al.* [29] have demonstrated the tuning efficacy of hybrid firefly pattern search (hFA-PS) algorithm in LFC area and show the superiority of hFA-PS over other existing control algorithms. A hybrid BFOA-PSO for the LFC study of linear and non-linear interconnected power system is presented in [30]. Guha *et al.* in his recent endeavour solved LFC problem using a krill-herd algorithm [31, 32]. TLBO algorithm is very much competitive over other optimisation techniques to show better performance for LFC system, but, in the learner phase, an adequate interaction between teachers and learners in the entire phase is not secured and the algorithm may enmesh in local optima. Besides these, moth-flame optimisation [33], dragonfly algorithm [34], differential search algorithm [35], JAYA algorithm [36] etc. are also successfully implemented in different areas of engineering and technology.

Though the aforesaid optimisation techniques show a significant improvement in the LFC performance, but the operation of these algorithms highly depends on the pre-definition of some input control parameters. For example, DE operation is entirely guided by the mutation factor and crossover rate. The probability to abandon a nest and scale factor is required for the operation of CSA. The operation of bat algorithm is highly susceptible to the selection of emission rate (r), loudness factor (A). In the case of HAS, determination of harmony memory consideration rate, pitch adjusting factor, and a number of improvisation are required. The input parameters of BBO algorithm are habitat modifications probability, initial mutation probability, maximum emigration rate, maximum immigration rate, step size of integration, lower and upper bounds for immigration probability. The TSA provides inferior results when search agent is far away from the global optimal position.

According to 'no-free-lunch' (NFL) theory, there is no optimisation technique, which is well suited for all optimisation problems. That means an optimisation technique gives satisfactory performance for a set of optimisation problems, but not for all. The NFL theory motivates researchers to search new optimisation technique to solve real-time optimisation problems. Hence, the possibility of exploring new optimisation technique is always acceptable if it is beneficial for LFC study. Having knowledge of the aforementioned discussion, a novel parameter free stochastic optimisation techniques namely multi-verse optimisation (MVO) [37] have been reported in this paper for the effective solution of LFC problem. This algorithm is derived by inspiring the multi-verse theory of physics. The main motivation of MVO is based on white hole, black hole, and wormhole of the universe. The main advantage of MVO algorithm is that its functionality only depends on the selection of population size (n_p) and maximum generation count (T). Additionally, it offers high convergence speed, easy to implement, straightforward, required less memory, and minimum computational cost. Literature review reveals that most of the reported works in LFC area are either considered two-area or three-area interconnected power plant, less attention has been paid on the study of four- or five-area power systems. Thus, based on the above discussion following are the main contributions of this paper:

- to model LFC dynamics of an interconnected power plant. Two test systems such as four-area hydrothermal and five-area thermal power plants are considered to narrate the dynamical performance of LFC.
- to take advantage of recently introduced stochastic optimisation algorithms namely MVO as an effective optimisation tool for the optimal design of LFC under the normal and perturbed scenario.
- to demonstrate the effectiveness and acceptability of the proposed control algorithms over other recently published algorithms, an extensive comparative study has been performed using transient analysis method.
- to study the effect of GRC and GDB on the system dynamics for the sake of robustness analysis.
- to projects a random load perturbation that may match the real-time load variation to judge the suitability of the designed controllers.
- to affirm the robustness of the suggested control schemes, loading, and parameter uncertainties are considered for analysis.

This paper is organised as follows: Section 2 describes the dynamic model of concerned power system with problem formulation. A brief description of MVO algorithm is presented in Section 3. Section 4 shows the algorithmic steps of proposed MVO algorithm to LFC problem. Simulation results and comparative analysis of the present work is presented and discussed in Section 5. Finally, Section 6 concludes the present work.

2 Problem formulation

2.1 System under study

The dynamic model of an interconnected power system model is enumerated under this heading. The investigated system comprises of four-area hydrothermal power plant as shown in Fig. 1*a* [6]. As viewed from Fig. 1*a* that area-1 and -2 are identical and of reheat-type thermal plant, while area-3 and -4 are hydro-type power plant with electrical governor. The nominal values of system parameters are taken from [6] and listed in Appendix (A.1). A step load increase of 1% in area-1 is chosen to appraise the dynamic stability of the studied power system. In Fig. 1*a*, R_i represents the speed regulation constant of governor, B_i is the frequency bias constant, T_{sg} is the hydraulic time constant, T_t is the turbine time constant, T_r is the reheat time constant, K_r is the reheat gain, K_{ps} is the control area gain, T_{ps} is the control area time constant, T_w is the water starting time of hydro-turbine, K_D, K_P, K_I are the electric governor derivative, proportional and integral gains, respectively, Δf_i is the frequency deviations in ith control area, $\Delta P_{tie,i,j}$ is the tie-line power deviation ith and jth control areas, and ΔP_D is the incremental change in system loading.

2.2 Proposed control structure

The main target of this simulation study is to identify the bounds of controller settings for which the system is remain in underdamped condition. Overdamped and critically damped systems are usually avoided because of its slow response and large time constant. In this article, an optimal PID controller is proposed, at the first instant, for LFC system because of its superior performance and

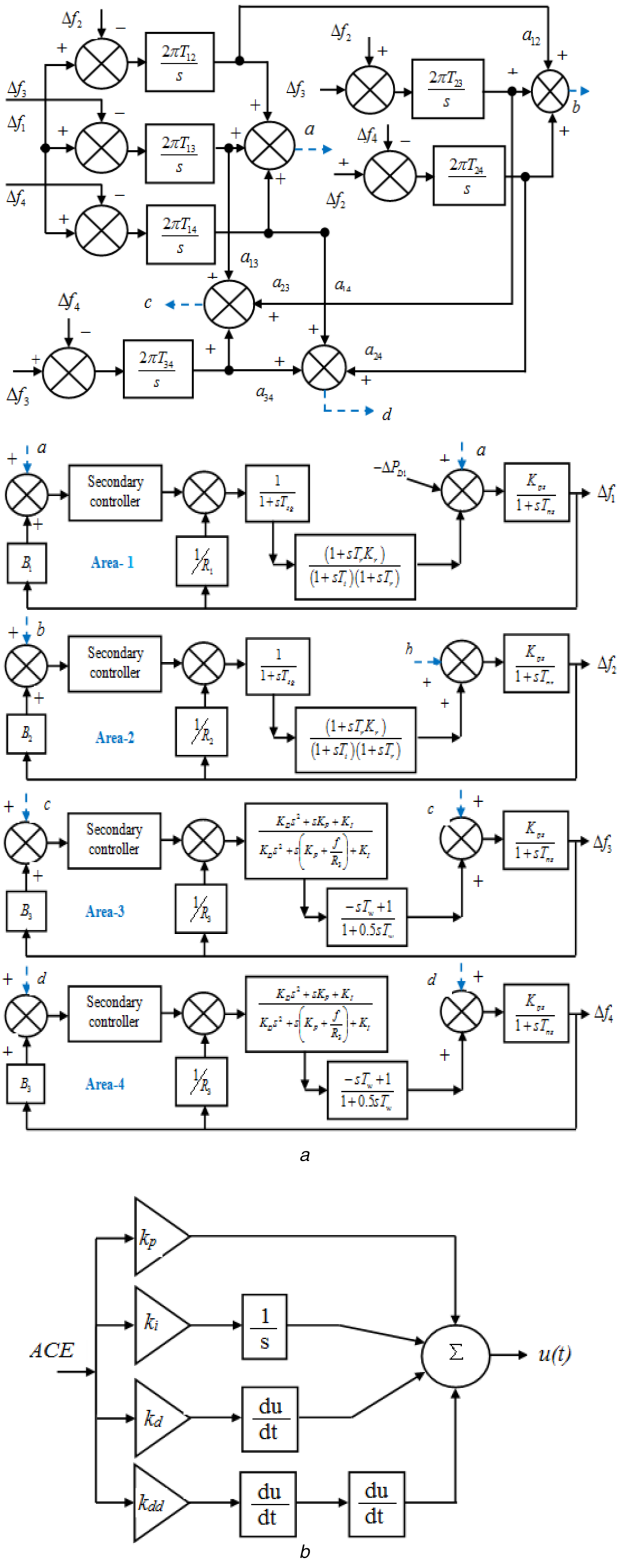

Fig. 1 *Four-area hydrothermal power plant*
(a) Transfer function model of four-area hydrothermal power plant, ***(b)*** Block diagram of PID + DD controller

higher degree of acceptability. Inputs to the PID controllers are the area control error (ACE_i) of the respective control area; here suffix i represents the number of control areas, i.e. 1, 2, 3, and 4. The controlled inputs (u_i) to the plant with PID-controller structure are defined as follows:

$$\mathrm{ACE}_i = B_i \Delta f_i + \Delta P_{\mathrm{tie},ij} \tag{1}$$

$$u_i = k_{\mathrm{p},i}\mathrm{ACE}_i + k_{\mathrm{i},i}\int \mathrm{ACE}_i + k_{\mathrm{d},i}\frac{\mathrm{d}}{\mathrm{d}t}(\mathrm{ACE}_i) \tag{2}$$

where $k_{\mathrm{p},i}$, $k_{\mathrm{i},i}$, and $k_{\mathrm{d},i}$ are the proportional, integral, and derivative controller gains of the ith control area, respectively. It is well known from the control system design that addition of 'zeros' to the system increase the damping factor and improves the degree of stability. In this article, double-derivative controller is integrated with PID controller and applied to individual control areas for better analysis of the current problem. The block diagram of PID + DD controller is shown in Fig. 1*b* [18]. The transfer function model of PID + DD controller is defined by

$$G_c(s) = k_{\mathrm{p}} + \frac{k_{\mathrm{i}}}{s} + sk_{\mathrm{d}} + s^2 k_{\mathrm{dd}} \tag{3}$$

where k_{dd} is the double-derivative gain.

The main objective of LFC is to nullify the ACE so as to restore the system stability after the disturbance. This is achieved by optimal tuning of secondary controllers. In optimal control theory, to extract the maximum benefits from the designed controller, objective function is first defined based on system specifications and constraints. In most the studied articles, integral square error (ISE), integral time square error (ITSE), integral absolute error, and integral time absolute error (ITAE)-based fitness function is defined for the design of secondary controllers. Among them ISE and ITAE have been widely used in the literature compared with ISE and ITSE. Therefore, in the current study authors have defined the fitness function based on ITAE criterion for tuning of PID and PID + DD controllers using MVO algorithm. The fitness function is defined as follows:

$$J = \int_0^T |(\mathrm{ACE}_i)| * t * \mathrm{d}t \tag{4}$$

One more factor that more or less affects the system performance is the range of unknown control variables. In the present study, the controller gains are selected between (0, 1). The proposed LFC problem can be viewed as a constraint optimisation problem bounded by the controller parameters. Thus, the optimisation problem can be defined as follows:

$$\text{minimise } J$$
$$\text{subjected to: } \begin{cases} k_{\mathrm{p,min}} \le k_{\mathrm{p}} \le k_{\mathrm{p,max}} \\ k_{\mathrm{i,min}} \le k_{\mathrm{i}} \le k_{\mathrm{i,max}} \\ k_{\mathrm{d,min}} \le k_{\mathrm{d}} \le k_{\mathrm{d,max}} \\ k_{\mathrm{dd,min}} \le k_{\mathrm{dd}} \le k_{\mathrm{dd,max}} \end{cases} \tag{5}$$

where $k_{\mathrm{pid,min}}$ and $k_{\mathrm{pid,max}}$ are the minimum and maximum values of PID-controller gains, respectively, $k_{\mathrm{dd,min}}$ and $k_{\mathrm{dd,max}}$ are the minimum and maximum limits of double-derivative block, respectively.

3 Multi-verse optimisation

3.1 Inspiration

In the line of 'big-bang theory', our universe starts with an immense explosion. The big-bang is the source of everything in this universe and there was nothing before that. The 'multi-verse theory' is another well-known and recently introduced theory between the physicists [37]. The American philosopher and psychologist William James coined the term multi-verse in 1895. The term multi-verse stands for 'opposite of universe' which allude to the existence of other universes including the universe that we are living in.

The multi-verse is a hypothetical set of a finite and an infinite number of universes including which we live. The main motivations of this optimisation technique are based on three notions of cosmology namely 'white hole', 'black hole', and 'wormhole' [37].

A white hole is never seen in the universe, but physicist believes that the big-bang can be considered as a white hole and may be the key factor for the birth of the universe. It is also

detected in multi-verse that the white holes are created because of the collisions of parallel universes. White holes are eruptions of matter and energy and nothing can get inside them. Physicist believes that the white holes are the possible outcomes to the law of general relativity.

A black hole behaves in contrast to a white hole, is a place in the universe where gravity pulls so much that a light cannot get out. This mainly happens because of the squeezed of matters into a tiny space. This can occur when a star is demised. Since no lights are getting out, we are unable to view the black holes.

A wormhole or Einstein-Rosen bridge is a hypothetical topological feature that would fundamentally be a shortcut connection between two distinct points in space–time. The American theoretical physicist Jhon Archibald Wheeler coined the term wormhole in 1957. However, the German mathematician Harman Weyl had proposed the said theory in 1921 based on the theory of electromagnetic field energy.

The inflation rate, was derived in the early 1980s, is another attribute of the universe for its expansion in space. Physicist believes that the inflation rate–speed is responsible for the formation of stars, planets, asteroids, black holes, white holes, wormholes, physical laws, and suitability for life. In the following subheadings, the mathematical model of proposed MVO algorithm is discussed.

3.2 Mathematical description of MVO algorithm

As stated before that the proposed MVO algorithm is mainly stimulated by the three main factors of cosmology, i.e. a white hole, black hole, and wormhole. In MVO algorithm, white holes and black holes are used to explore the search space and wormhole assists MVO algorithm in exploiting the search space [37]. Each solution in MVO algorithm is analogous to universe and variables of the solutions are the object of that universe. In MVO algorithm, the inflation rate is similar to the fitness value of the candidate solution. In [37], following assumptions were made to from the MVO algorithm:

(i) Higher the inflation rate, higher probability of getting large numbers of white holes in the universes.
(ii) Higher the inflation rate, lower probability of having black holes in the universes.
(iii) Universes with higher inflation rate tend to send the objects through white holes.
(iv) Universes with higher inflation rate tend to receive the objects through black holes.
(v) The objects in all the universes may face random movement towards the best universe through wormholes irrespective to the inflation rate.

To develop the mathematical model of white/black holes tunnels and exchange the objects between the universes, Mirjalili *et al.* [37] proposed roulette wheel mechanism to select the best universe. During the entire course of a generation, the candidate solutions are sorted and roulette wheel theory is applied to select the best solution. The best solutions will be treated as white holes.

Let the universe is randomly defined in the solution space and stored in the following matrix:

$$\boldsymbol{U} = \begin{bmatrix} X_1^1 & X_1^2 & . & X_1^j & . & X_1^d \\ X_2^1 & X_2^2 & . & X_2^j & . & X_2^d \\ . & . & . & . & . & . \\ X_i^1 & X_i^2 & . & X_i^j & . & X_i^d \\ . & . & . & . & . & . \\ X_n^1 & X_n^2 & . & X_n^j & . & X_n^d \end{bmatrix} \tag{6}$$

where $\boldsymbol{U}$ is the universe, n is the number of search elements, d is the dimension of control variables, X_i^j is the jth parameter of ith universe which is defined as follows:

$$X_i^j = \begin{cases} X_k^j & if \quad r_1 < NI(U_i) \\ X_i^j & r_1 \geq NI(U_i) \end{cases} \tag{7}$$

where U_i is the ith universe, NI is normalised inflation rate, r_1 random number selected between $[0, 1]$, X_k^j is the jth parameter of kth universe selected based on roulette wheel mechanism.

The pseudo code for exploring the best universe via roulette wheel selection mechanism is described in Algorithm 3.1 [37] (Fig. 2).

To maintain the diversity of universes and to perform the exploitation theory, wormholes are considered in each universe to transport the objects randomly through space without considering the inflation rate. The formation of wormhole to exploit the search ability in MVO algorithm is defined by the following pseudo code:

$$X_i^j = \begin{cases} \begin{cases} X_j + \text{TDR} * \left((ub_j - lb_j) * r_4 + lb_j \right) & r_3 < 0.5 \\ X_j - \text{TDR} * \left((ub_j - lb_j) * r_4 + lb_j \right) & r_3 \geq 0.5 \end{cases} & r_2 < \text{WEP} \\ X_i^j \quad r_2 \geq \text{WEP} \end{cases} \tag{8}$$

where X_j indicates the jth parameter of best universe obtained so far, TDR (traveling distance rate) and WEP (wormhole existence probability) are two constants, ub and lb are the upper and lower bound of the jth parameter, r_2, r_3 and r_4 are randomly generated number between $[0, 1]$.

The WEP is the coefficient for defining the probability of the existence of wormholes in the universe and calculated using (9). The coefficient WEP is responsible for enhancing the exploitation property of the optimisation problem

$$\text{WEP} = \min + t * \left(\frac{\max - \min}{T} \right) \tag{9}$$

where t is the current iteration, T is the maximum number of iteration, min and max are the minimum and maximum values of the controlled variables.

Travelling distance rate (TDR) is another important attribute in MVO algorithm to define the distance rate so that an object can be teleported by a wormhole around the universe. The coefficient TDR is calculated using (10)

$$\text{TDR} = 1 - \frac{t^{(1/p)}}{T^{(1/p)}} \tag{10}$$

where p is the exploitation accuracy over the iteration. High the value of p, more accurate exploitation ability. Algorithm 3.2 (see Fig. 3) is employed to update the current position of search agents.

The general flowchart of proposed MVO algorithm is available in Fig. 4*a*.

4 MVO applied to LFC problem

Different steps of LFC-based MVO algorithm is mentioned as follows:

Step 1: Initialise the universes (controller gains in LFC study) randomly within the search space and calculate the inflation rate (ACE value) of the individual universe by (4).
Step 2: Initialise minimum and maximum WEP, i.e. $\text{WEP}_{\min} = 1$ and $\text{WEP}_{\max} = 0.2$. Best universe, $U_{\text{best}} = \text{zeros}(1, \text{dim})$, and best universe inflation rate, $\text{IR}_{\text{best}} = \inf$.
Step 3: Compute WEP and TDR using (9)and (10), respectively.
Step 4: Check whether the generated solutions are within the search limit or not.
Step 5: Sort the population from best to worst based on the inflation rate, ACE value, calculated in Step 1.

Step 6: Find out the elite solution employing following pseudo code:

if $\text{IR}(1,i) < \text{IR}_{\text{best}}$

$\text{IR}_{\text{best}} = \text{IR}(1,i);$

$U_{\text{best}} = U(1,:);$

end

Step 7: Calculate the normalised inflation rate using Algorithm 3.1 (Fig. 2).

Step 8: Update the position of search agents (controller gains) employing Algorithm 3.2 (Fig. 3).

Step 9: Calculate the inflation rate (ACE value) using (4) for the newly generated solutions and sort the population from best to worst.

Step 10: Go to Step 7 until the termination criterion is met.

Step 11: Print the best optimal solutions of controller gains and calculate typical transient specifications to identify the degree of relative stability.

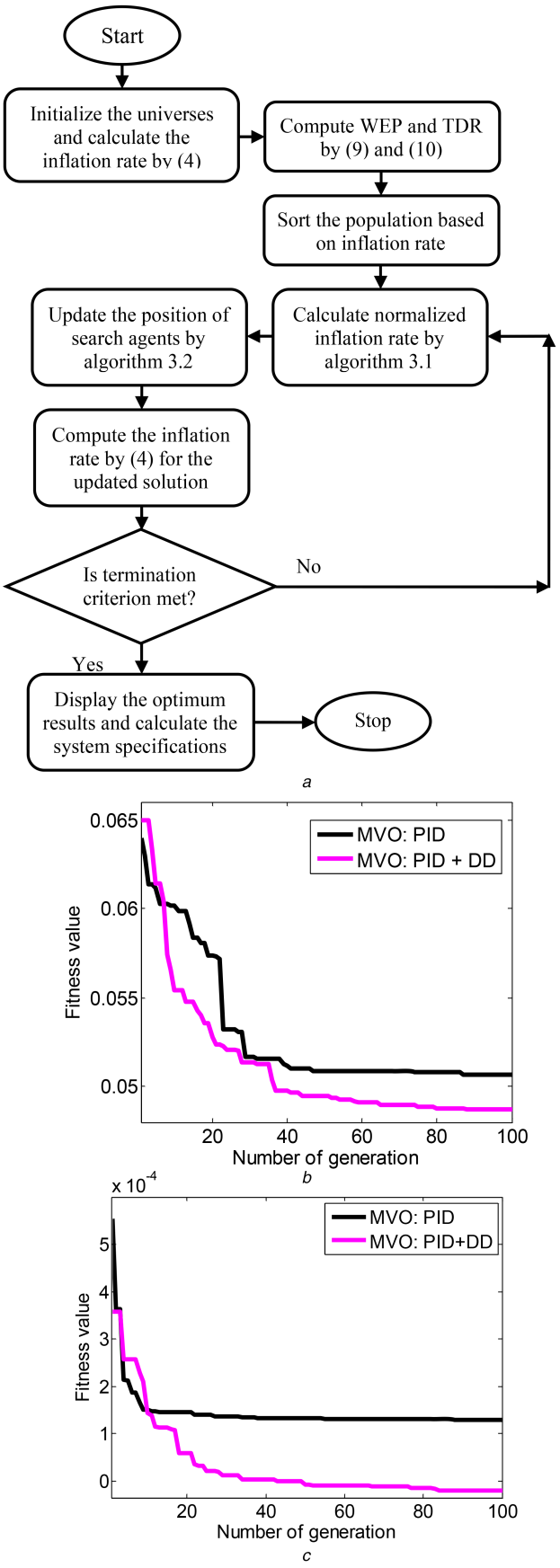

Fig. 2 *Algorithm: 3.1*

5 Simulation results and discussions

For any control process, quick response and higher degree of stability are enviable. It is remarkable that lower the performance indices, better the time-domain specifications and higher the degree of relative stability. Under this heading, critical investigation of power system dynamics has been done and the acceptability of the designed controller is established by computing peak overshoot and settling time of the transient responses. The dynamic and static system stability of the concerned power systems are examined after small step load perturbation (SLP). The size and location of SLP for stability analysis is discussed in their respective heads. The simulation model of test system has been developed in SIMULINK environment, while the optimisation code is separately written in.*m* file. The simulations were performed in an Intel core i3 processor of 2.4 GHz and 2 GB RAM in MATLAB 7.10.0.499 (R2009a) environment. The major observation of the current study is highlighted in the following headings and marked by italic faces. The obtained results are best in terms of minimum fitness value and minimum transient specifications.

Owing to the random nature of optimisation technique, different trails have been made to select the input parameters of MVO algorithm. The operation of MVO is only required initialisation of population size and maximum iteration count. Eleven different values of population size are considered to assess the performance of MVO in the present problem. The final control parameters and corresponding fitness value are offered in Table 1. It is observed from Table 1 that minimum fitness value (*ITAE = 0.0507*) is achieved with $n_{\text{p}} = 40$. It is also remarkable from Table 1 that higher value of n_{p} degrades the system performance. The convergence profile of proposed algorithm with PID and PID + DD controllers for test system 1 is depicted in Fig. 4*b*. It is noteworthy from Fig. 4*b* that PID + DD controller converges to optimal solution at a faster rate than that of PID controller and takes 80–90 iterations to reach the global point. This also justifies the choice of maximum iteration count, i.e. 100 for present study. Thus the population size and maximum iterations are set to 40 and 100, respectively, for the present study.

5.1 Transient analysis of test system-1

In this section, the dynamic performance of test system-1 subjected to 1% SLP in area-1 has been investigated. Initially, the test system-1 as shown in Fig. 1*a* is studied with PID controllers. The proposed MVO algorithm is employed to search near global optimal solutions of PID controllers. The optimal controller settings with fitness value are provided in Table 1. To show the superiority, the results of MVO algorithm is compared with DE algorithm and other control algorithms reported in [6] for identical power system. However, the control variables computed by the above methods are not shown in this paper. The comparative results are shown in Fig. 5. Typical transient specifications such as peak overshoot and settling time of disperse states of test system-1 are calculated from Fig. 5 and shown in Table 2. It is seen from Fig. 5 that the system oscillations are poorly damped with ANN-,

NI : Normalized inflation rate of the universes
SU : Sorted universes
for $i = 1 : n_p$
$black\_hole\_index = i;$
for $j = 1 : \dim$
$r_1 = rand(0,1);$
if $r_1 < NI(U_i)$
$white\_hole\_index =$
$RouletteWheelSelection(-NI);$
$U(Black\_hole\_index, j)$
$= SU(white\_hole\_index, j);$
end
end
end

Fig. 3 *Algorithm: 3.2*

for $i = 1 : n_p$;
for $j = 1 : \dim$;
$r_2 = rand(0,1)$;
if $r_2 < WEP$
$r_3 = rand(0,1); r_4 = rand(0,1);$
if $r_3 < 0.5$
$U(i,j) = U_{best}(j) + TDR*(ub(j) - lb(j))*r_4 + lb(j)$;
else
$U(i,j) = U_{best}(j) - TDR*(ub(j) - lb(j))*r_4 + lb(j)$;
end
end
end
end

Fig. 4 *MVO algorithm*
(a) Flowchart of MVO algorithm, ***(b)*** Convergence characteristic of MVO algorithm for Test system-1, ***(c)*** Test system-2

Table 1 Comparative study of MVO algorithm with different population size (test system-1)

Population size, n_p	Area-1			Area-2			Area-3			Area-4			J
	k_{pl}	k_{il}	k_{dl}	k_{p2}	k_{i2}	k_{d2}	k_{p3}	k_{i3}	k_{d3}	k_{p4}	k_{i4}	k_{d4}	
10	0.5218	0.9715	0.0914	0.7165	0.9971	0.4948	0.1838	0.5784	0.4539	0.2066	0.5403	0.6555	0.0544
15	0.8911	0.9381	0.2799	0.9350	0.9780	0.1851	0.9367	0.4619	0.4091	0.9595	0.0154	0.2158	0.0524
20	0.9536	0.9954	0.1263	0.9757	0.9319	0.3235	0.8538	0.1442	0.5614	0.8935	0.3253	0.1245	0.0519
25	0.9161	0.9953	0.2383	0.6972	0.9477	0.2110	0.2892	0.3709	0.2124	0.5401	0.1162	0.4849	0.0528
30	0.8751	0.9559	0.2097	0.9775	0.9864	0.2501	0.9004	0.3183	0.2228	0.9441	0.1457	0.4749	0.0517
35	0.9866	0.9884	0.2624	0.9087	0.9717	0.1695	0.8762	0.0829	0.0289	0.9522	0.3859	0.7334	0.0512
40	**0.9844**	**0.9994**	**0.1260**	**0.9803**	**0.9756**	**0.3600**	**0.9119**	**0.4964**	**0.3437**	**0.9525**	**0.0099**	**0.3517**	**0.0507**
45	0.9857	0.9743	0.2951	0.8484	0.9806	0.1785	0.8442	0.2172	0.4701	0.9605	0.2501	0.0714	0.0514
50	0.9848	0.9849	0.3662	0.9792	0.9552	0.1015	0.6353	0.0691	0.4262	0.9560	0.4031	0.3449	0.0516
55	0.9533	0.9318	0.2148	0.9699	0.9729	0.2360	0.6822	0.4089	0.2262	0.8567	0.1011	0.6015	0.0528
60	0.9552	0.8867	0.1149	0.8547	0.9640	0.3355	0.8320	0.2945	0.5332	0.8629	0.1682	0.1161	0.0543

Bold face values show the best value.

FLC-, and DE-based controllers. However, settling time of frequency and tie-line power oscillations is small with MVO-tuned PID controller compared with DE-, FLC-, ANN-, and ANFIS-based intelligent controllers. This helps to conclude that MVO has better tuning ability and provide more optimal controllers for the LFC study. It is remarkable from Table 2 that MVO-tuned PID controller provides the output with high peak overshoot compared with DE-tuned PID controller for the same test system. It is worth mentioning that minimisation of settling time and peak overshot is simultaneously not possible.

Now to accelerate the system performance, PID + DD controllers are optimally designed and placed in the control areas. The MVO algorithm is used to set the controller settings employing ITAE-based fitness function. Same procedure as described in Section 4 is followed to search the control variables of PID + DD controllers. The tunable parameters of PID + DD controller are, *area-1*: $k_{p1} = 0.8726$, $k_{i1} = 0.9953$, $k_{d1} = 0.3381$ and $k_{dd1} = 0.0774$, *area-2*: $k_{p2} = 0.7686$, $k_{i2} = 0.9966$, $k_{d2} = 0.2432$ and $k_{dd2} = 0.0102$, *area-3*: $k_{p3} = 0.8767$, $k_{i3} = 0.1223$, $k_{d3} = 0.5037$ and $k_{dd3} = 0.1161$, *area-4*: $k_{p4} = 0.9050$, $k_{i4} = 0.3461$, $k_{d4} = 0.2815$ and $k_{dd4} = 0.0493$. The corresponding fitness value is *ITAE = 0.0489*. It is to be noted that fitness value is further reduced by *3.55%* with MVO-tuned PID + DD controller compared with MVO-tuned PID controller. The comparative system dynamics of this studied system is shown in Fig. 6. It is noteworthy from Fig. 6 that MVO-tuned PID + DD controllers provide high damping to the system oscillations and restore the system stability at a faster rate compared with MVO-tuned PID controllers. The peak overshoot, undershoot and settling time of system responses are found to be less with MVO-tuned PID + DD controller. Based on the above discussion, it is concluded that PID + DD controller outperformed PID controller.

5.1.1 Robustness study of test system-1: To check the feasibility of the designed controller, a random load pattern (RLP) as shown in Fig. 7 (marked by the blue colour line) is applied to area-1. The MVO-tuned PID + DD controllers are used in this case because of its beneficial performance compared with others. The load perturbation is random both in magnitude and time [12]. The closed loop system responses subjected to RLP are shown in Fig. 7. It is seen from Fig. 7 that designed controller is able to maintain the system stability and extenuate the effects of load perturbation from the frequency and tie-line power quickly. It is also noteworthy from Fig. 7 that designed controllers provide an adequate damping to the system oscillations and restore the frequency and tie-line power to its steady value even in the presence of RLP. Thus the robustness of the controller is believed.

5.1.2 Sensitivity analysis: To demonstrate the robustness of designed PID + DD controllers, the sensitivity analysis is carried out under the parametric uncertainty conditions. The system parameters are changed in the range of +25 to − 25% [29] without changing the PID + DD controller gains. The varied system parameters are $T_t, T_{sg}, K_{ps}, T_{ps}, K_r$ and T_r. The minimum ITAE value and settling time under normal and perturbed conditions are given in Table 3. Critical review of Table 3 reveals that system performances are merely changes with the proposed algorithm and the effect of these variations on the system dynamics can be

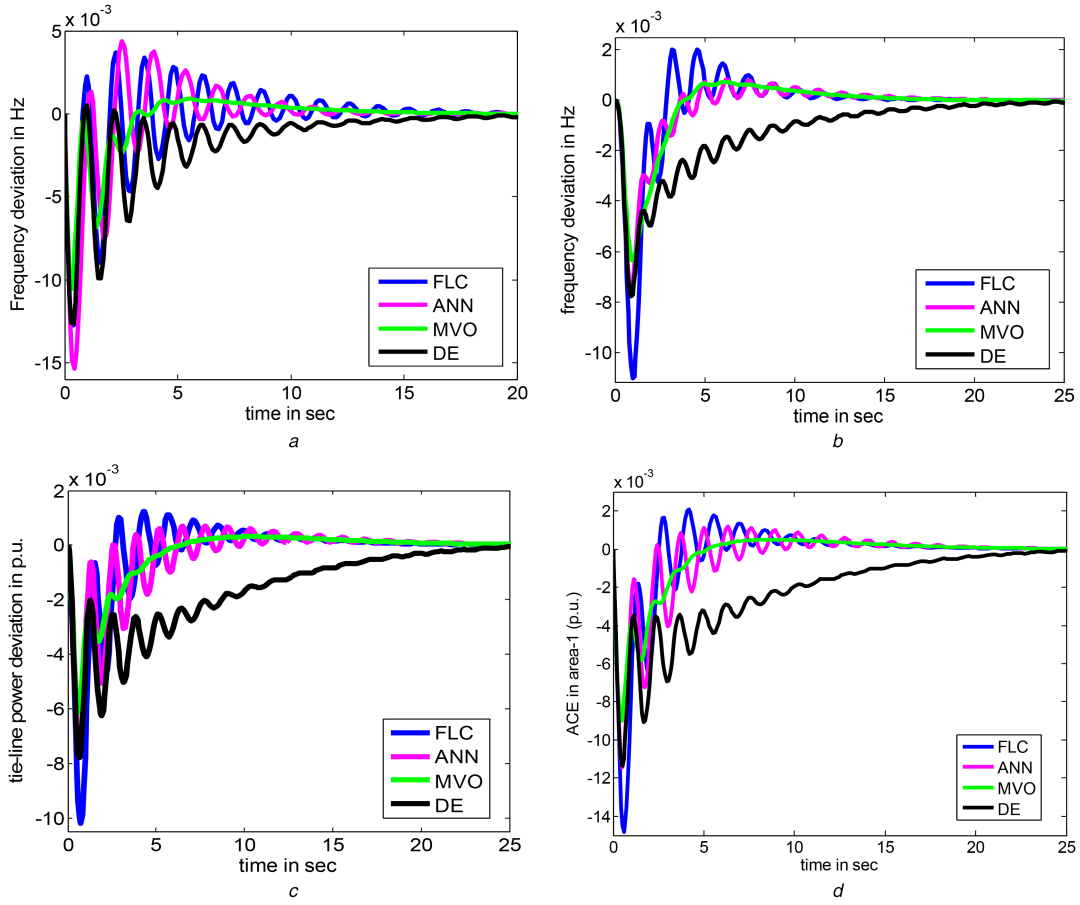

Fig. 5 *Dynamic performance of test system-1 with PID controllers*
(a) Change of frequency in area-1, ***(b)*** Change of frequency in area-2, ***(c)*** Change of tie-line power between thermal areas, ***(d)*** Change of ACE of area-1

Table 2 Comparative system performance of test system-1 with MVO algorithm

Transient specifications		Overshoot						Settling time, s					
		Δf_1	Δf_2	Δf_3	Δf_4	$\Delta P_{tie,th-th}$	$\Delta P_{tie,th-hy}$	Δf_1	Δf_2	Δf_3	Δf_4	$\Delta P_{tie,th-th}$	$\Delta P_{tie,th-hy}$
Ref. [6]	PI	0.055	0.055	0.067	0.066	0.0145	0.05	64	64	70	65	65	70
	PID	0.049	0.049	0.057	0.062	0.005	0.0042	60	60	60	50	62	60
	Fuzzy	0.059	0.06	0.068	0.065	0.005	0.012	45	45	45	48	40	45
	ANN	0.038	0.038	0.055	0.051	0.006	0.013	40	40	40	40	30	35
	ANFIS	0.061	0.061	0.054	0.054	0.0052	0.045	18	18	17	17	15	27
proposed	MVO	0.0043	0.0020	0.0020	0.0019	0.0012	0.0034	**11.2**	**11.9**	**11.8**	**11.6**	**14.34**	**15.82**
	DE	**4.84×10^{-4}**	**8.18×10^{-5}**	**1.65×10^{-5}**	**4.05×10^{-5}**	**6.96×10^{-5}**	**0.0025**	18.6	25.9	21.5	24.03	23.18	23.99

Bold face values show the best value.

neglected. Thus, it can be concluded that the designed controller is robust and need not be reset while system parameters are changed.

5.2 Transient analysis of test system-2

To demonstrate the tuning efficacy, the simulation study is forwarded to another complex and non-linear power system with distinct secondary controllers. The investigated system is comprised of five unequal thermal power plants of area-1: 2000 MW, area-2: 4000 MW, area-3: 8000 MW, area-4: 10,000 MW and area-5: 12,000 MW [4]. Each area consists of single-stage reheat turbine. To add some degree of non-linearity, GRC of 3%/min in each area is included in the simulation study. The linear approximated model of test system-2 is shown in [4]. The nominal values of system parameters are given in the Appendix. The proposed PID and PID + DD controllers are individually employed in each control area to assess the dynamic stability of test system-2 after the load variation. The MVO algorithm is used to search near global optimum settings of said controllers via the minimisation of ISE-based fitness function as defined in (11). The same procedures as discussed in 'Section 4' are followed to set the parameters of PID and PID + DD controllers. The controller gains are selected between (0, 1)

$$J_{\mathrm{ISE}} = \int_0^T (\mathrm{ACE}_i)^2 \, \mathrm{d}t, \quad i = 1, 2, 3, 4, 5 \tag{11}$$

At the first instant, PID controllers are integrated into the control areas and its effect on the system performance is investigated. The optimum PID-controller gains with MVO algorithm is offered in Table 4. Minimum fitness value computed with MVO-tuned PID controller is $ISE = 1.3610 \times 10^{-4}$. To show the supremacy, the results of MVO algorithm are compared with DE and BFOA [4] algorithms. However, the controller gains computed by the above methods are not shown in this article. The dynamic performance of the concerned power system subjected to 1% SLP in area-1 is shown in Fig. 8. The settling time and peak overshoot of frequency and tie-line power deviations are noted from Fig. 8 and listed in Table 4. For better comparison, the output results of BFOA and DE are also offered in Fig. 8. A critical

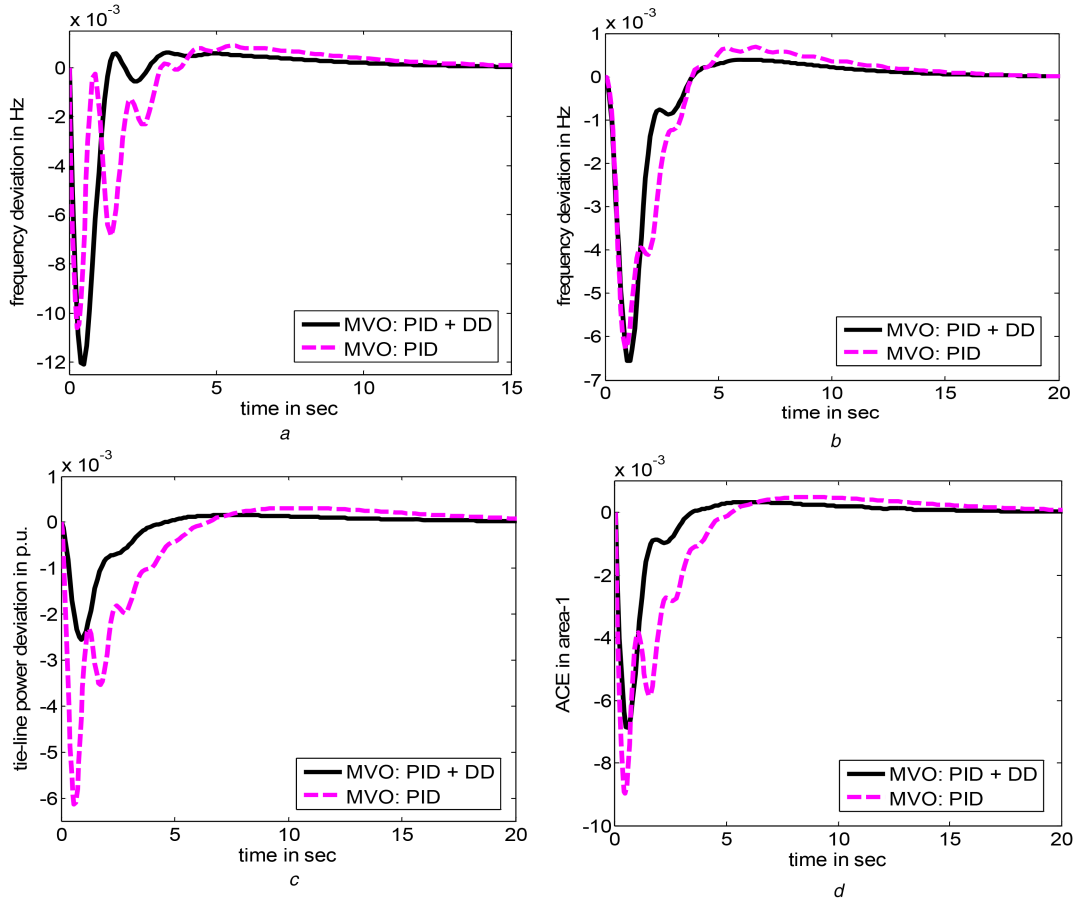

Fig. 6 *Dynamic performance of test system-1 after 1% SLP in area-1*
(a) Change of frequency in area-1, ***(b)*** Change of frequency in area-2, ***(c)*** Change of tie-line power between thermal areas, ***(d)*** Change of ACE in area-1

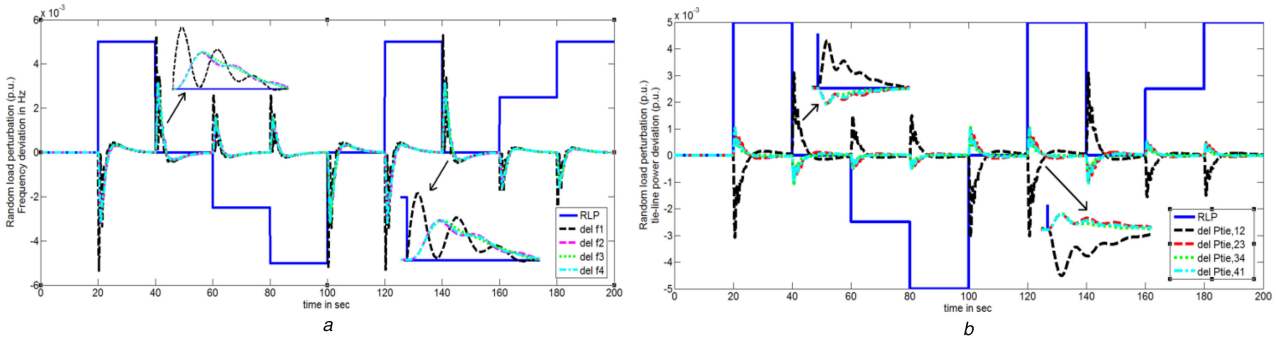

Fig. 7 *Dynamic performance of test system-1 with RLP*
(a) Change of frequency in area-1, ***(b)*** Change of tie-line power

review of Fig. 8 shows that proposed MVO-tuned PID controllers provide better outputs compared to BFOA and DE algorithms.

To ameliorate the system dynamics, PID + DD controller is included in the controlled areas in lieu of PID controllers. The optimum controller gains calculated by MVO algorithm are shown in Table 4. It is noteworthy from Table 4 that minimum fitness value is decreased with PID + DD controllers ($ISE = 9.8416 \times 10^{-5}$) and improved by *27.69%*. The comparative convergence characteristic for test system-2 is shown in Fig. 4*b*. It is also remarkable from Fig. 4*b* that MVO-tuned PID + DD controller approaches to the optimal point at a faster rate compared to MVO-tuned PID controller. The dynamic responses of test system-2 system with MVO-tuned PID + DD controllers are sketched in Fig. 8. It is remarkable from Fig. 8 that the system oscillations are effectively died out with PID + DD controllers. Also, compared to PID controllers, the proposed MVO-tuned PID + DD controllers offer minimum settling time and less peak overshoot. Thus, it may be inferred from the above discussion that designed PD + PID controller is much faster than MVO-tuned PID controller and effectively enhance the system stability.

5.2.1 Extended to non-linear system: To verify the feasibility of MVO algorithm, GDB non-linearity is added to the system and its impact on the system dynamics has been examined. The controller gains obtained at nominal conditions as given in Table 4 are considered to assess the system stability. The closed loop system responses with GDB are shown in Fig. 9. To demonstrate the superiority of MVO-tuned PID + DD controller, the closed loop responses are compared with MVO-tuned PID controllers. It is mentionable from Fig. 9 that the test system with PID controller possesses more oscillation with high peak overshoot and takes more time to settle down. Conversely, responses with PID + DD controller effectively attenuated and drive back to steady value at a faster rate. Further the designed PID + DD controller effortlessly mitigates the effects of GDB and improves the degree of stability. Hence, it may conclude that PID + DD controller outperformed PID controller. Further, the robustness of the MVO-tuned PID + DD controller is validated.

Table 3 Sensitivity analysis of test system-1

Parameters	% of change	ITAE value	Settling time, s					
			Δf_1	Δf_2	Δf_3	Δf_4	$\Delta P_{tie,th-th}$	$\Delta P_{tie,th-hy}$
Nominal	No. of change	0.0507	11.2	11.9	11.8	11.6	14.34	15.82
T_t	+25	**0.0514**	**15.7**	**14.92**	**14.92**	**14.87**	**17.5**	**18.9**
	−25	0.0510	9.74	11.53	11.4	11.46	13.89	15.81
K_r	+25	0.0388	9.37	11.14	10.07	10.08	12.43	12.16
	−25	0.0681	13.82	12.43	12.43	12.43	16.45	18.01
T_r	+25	0.0557	12.43	13.13	13.11	13.08	15.60	17.23
	−25	0.0276	11.09	10.5	10.49	10.49	12.97	14.36
T_{sg}	+25	0.0510	13.87	13.22	13.21	13.19	15.69	17.14
	−25	0.0506	9.94	11.74	11.63	10.75	13.35	15.8
K_{ps}	+25	0.0502	11.03	11.65	11.64	11.62	13.96	15.32
	−25	0.0515	13.05	12.34	12.33	12.33	15.18	16.82
T_{ps}	+25	0.0513	12.63	11.93	11.93	11.93	14.71	16.33
	−25	0.0501	10.68	11.31	11.29	11.29	13.56	15.79
R_i	+25	0.0520	11.41	12.02	11.99	11.98	14.58	16.07
	−25	0.0486	10.89	11.62	11.62	11.62	14.05	15.50
B_i	+25	0.0516	9.77	10.53	10.51	10.53	13.94	15.76
	−25	0.0494	14.05	13.37	13.37	13.35	15.82	17.25
loading	+25	0.0633	11.21	11.86	11.86	11.85	14.35	15.82
	−25	0.0380	11.19	11.87	11.85	11.85	14.34	15.81

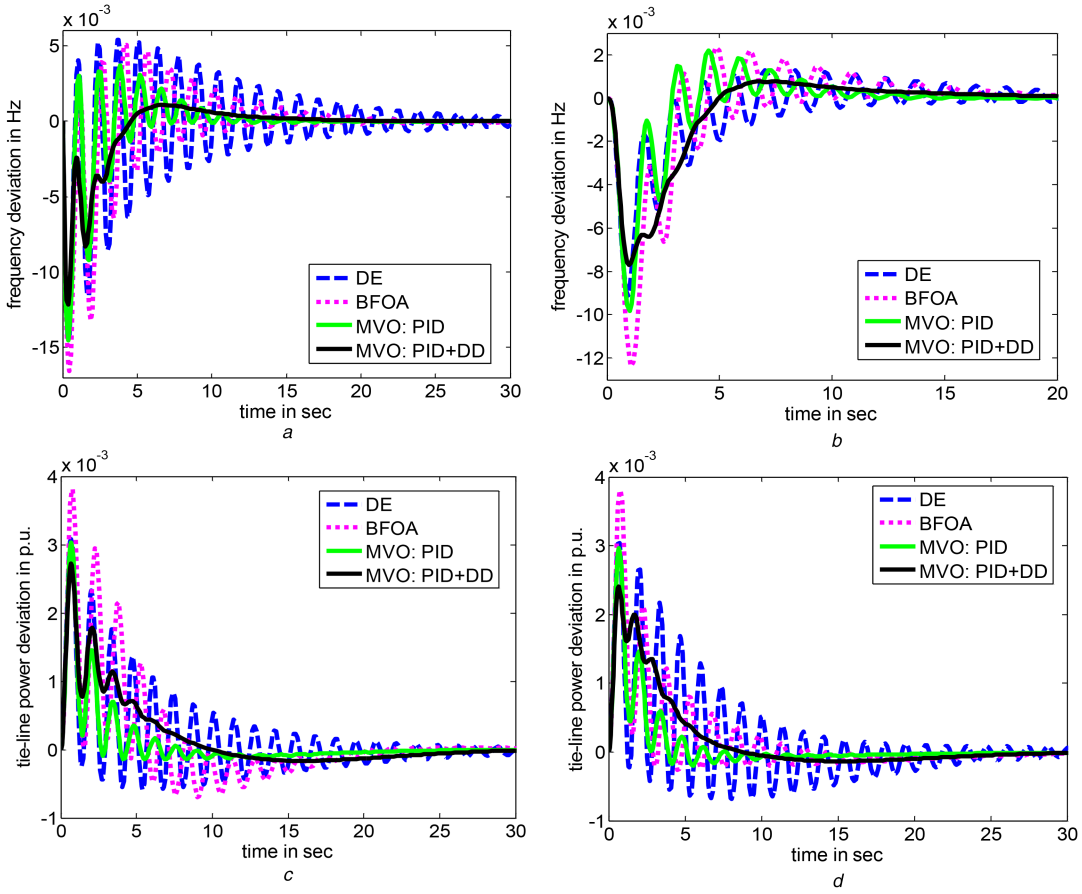

Fig. 8 *Dynamic performance of test system-2 with GRC*
(a) Change of frequency in area-1, ***(b)*** Change of frequency in area-3, ***(c)*** Change of tie-line power $\Delta P_{tie,23}$, ***(d)*** Change of tie-line power $\Delta P_{tie,45}$

5.2.2 Robustness analysis of test system-2: To affirm the robustness of PID + DD controllers for test system-2, same random load profile as considered for test system-1 is applied to area-1. The change of frequency and tie-line power with this RLP is shown in Fig. 10. Fig. 10 helps to infer that designed controllers effectively handle this situation and gives satisfactory output. The investigation also reveals that power system does not lose its stability under the action of RLP.

6 Conclusion

In the present work, LFC of an interconnected power system comprising of four- and five-area have been established through time-domain simulation. The dynamic behaviour of concerned power systems with PID and PID + DD controllers is inspected and compared. The optimal gains of the said controllers have been searched by MVO algorithm via the minimisation of ISE- and ITAE-based fitness functions. To corroborate the advantage and

Table 4 Optimal controller gains for test system-2 with MVO algorithm

Control algorithms		Area-1	Area-2	Area-3	Area-4	Area-5	Fitness value
MVO: PID	k_p	0.7962	0.5830	0.1335	0.1929	0.8975	1.3610×10^{-4}
	k_i	0.9772	0.9496	0.7871	0.1049	0.4966	
	k_d	0.1881	0.9641	0.7898	0.0891	0.8042	
	peak overshoot	**0.0089**	0.0205	**0.0075**	$\mathbf{1.49 \times 10^{-4}}$	**0.0059**	
	settling time, s	18.66	16.74	18.45	19.05	21.04	
MVO: PID + DD	k_p	0.9656	0.8109	0.8091	0.8022	0.3590	$\mathbf{9.8416 \times 10^{-5}}$
	k_i	0.7055	0.2189	0.6700	0.9293	0.5856	
	k_d	0.9518	0.2669	0.4031	0.4269	0.3626	
	k_{dd}	0.7336	0.3148	0.0117	0.8168	0.2659	
	peak overshoot	0.0198	$\mathbf{7.50 \times 10^{-4}}$	0.0287	0.0121	0.0128	
	settling time, s	**16.32**	**13.82**	**17.94**	**17.41**	**17.61**	

Bold face values show the best results.

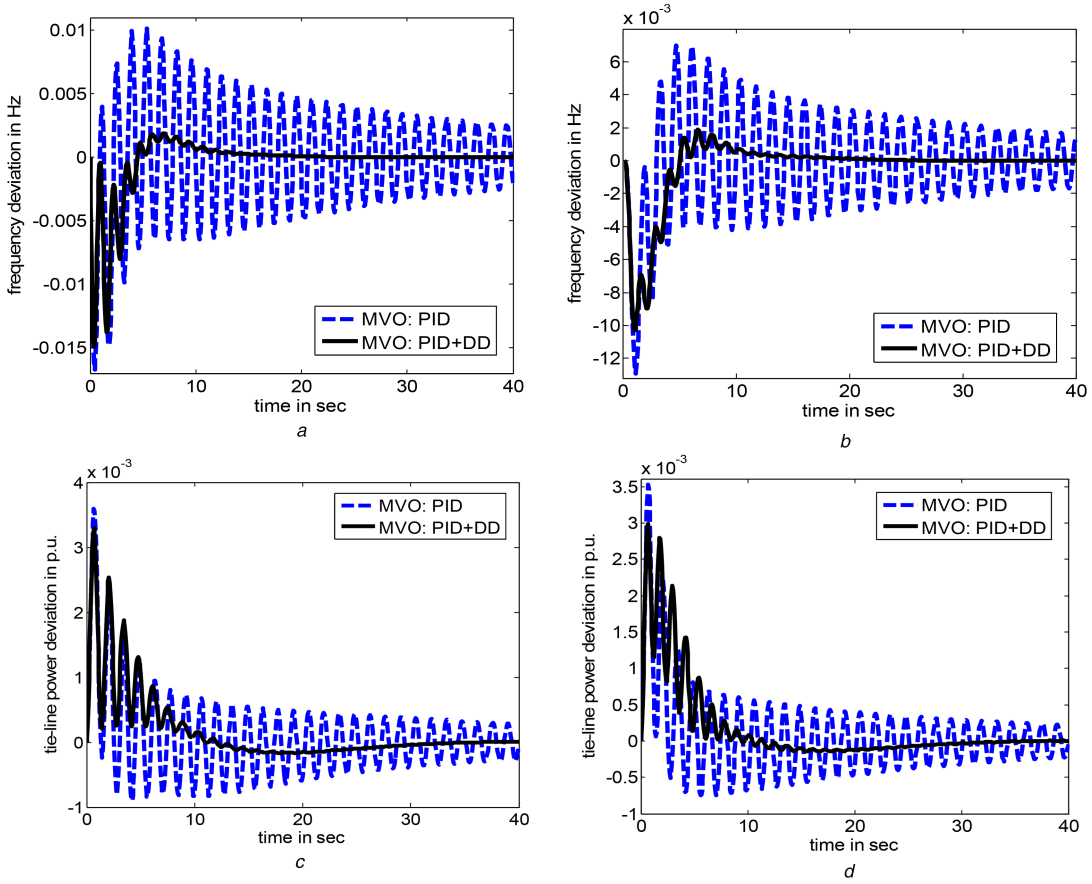

Fig. 9 *Dynamic performance of test system-2 with GRC and GDB*
(a) Change of frequency in area-1, ***(b)*** Change of frequency in area-3, ***(c)*** Change of tie-line power $\Delta P_{tie,23}$, ***(d)*** Change of tie-line power $\Delta P_{tie,45}$

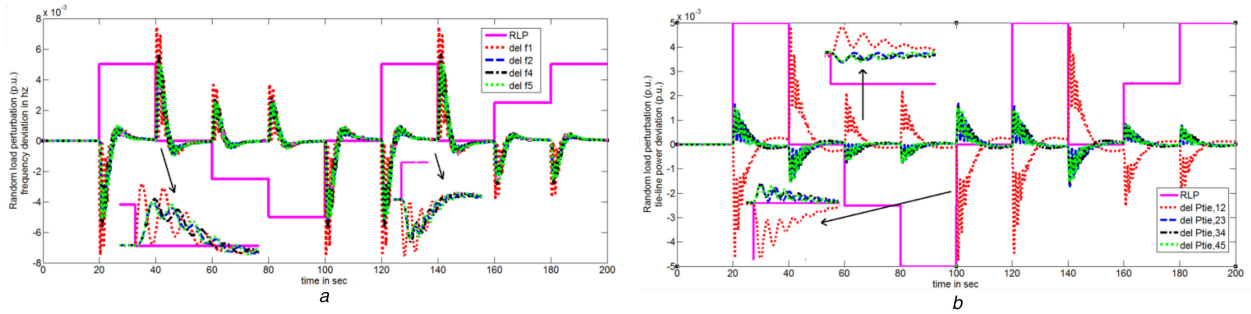

Fig. 10 *Dynamic performance of test system-2 with RLP*
(a) Change of frequency in area-1, ***(b)*** Change of tie-line power

potential benefits yielded by the designed controllers, the closed loop results of MVO algorithm are compared with DE-, BFOA-, FLC-, ANN- and ANFIS-based intelligent controllers. Numerical results and the convergence profile show that designed PID + DD

controller offers better system output compared to others. Robustness of the deigned controller is believed under RLP and parametric uncertainty conditions. Simulation results confirm the efficacy and robust performance of the proposed MVO algorithm in bringing frequency stability effortlessly subjected to disturbances.

7 References

[1] Yesil, E., Guzelkaya, M., Eksin, I.: 'Self-tuning fuzzy PID type load and frequency controller', *Energy Convers. Manage*, 2004, **45**, pp. 377–390

[2] Guha, D., Roy, P.K., Banerjee, S.: 'Load frequency control of large power system using quasi-oppositional grey wolf optimization algorithm', *Int. J. Eng. Sci. Technol.*, 2016, **19**, (4), pp. 1693–1713

[3] Pandey, S.K., Mohanty, S.R., Kishore, N.: 'A literature review on LFC for conventional and distributed generation power system', *Renew. Sustain. Energy Rev.*, 2013, **25**, pp. 318–324

[4] Saikia, L.C., Nanda, J., Mishra, S.: 'Performance comparison of several classical controllers in AGC for multi-area interconnected thermal system', *Int. J. Elect. Power Energy Syst.*, 2011, **33**, pp. 394–401

[5] Saikia, L.C., Sinha, N., Nanda, J.: 'Maiden application of bacterial foraging based fuzzy IDD controller in AGC of a multi-area hydrothermal system', *Int. J. Elect. Power Energy Syst.*, 2013, **45**, pp. 98–106

[6] Prakash, S., Sinha, S.K.: 'Simulation based neuro-fuzzy hybrid intelligent PI control approach in four-area load frequency control of interconnected power system', *Appl. Soft Comput.*, 2014, **23**, pp. 152–164

[7] Yousef, H.: 'Adaptive fuzzy logic load frequency control of multi-area power system', *Int. J. Elect. Power Energy Syst.*, 2015, **68**, pp. 384–395

[8] Tripathy, S.C., Hope, G.S., Malik, O.P.: 'Optimisation of load-frequency control parameters for power systems with reheat steam turbines and governor dead band nonlinearity', *IEE Proc.*, 1982, **129**, (1), pp. 10–16

[9] Tripathy, S.C., Bhatti, T.S., Jha, C.S., *et al.*: 'Sampled data automatic generation control analysis with reheat steam turbines and governor dead band effects', *IEEE Trans. Power Apparatus Syst.*, 1984, **PAS-103**, (5), pp. 1045–1051

[10] Guha, D., Roy, P.K., Banerjee, S.: 'Load frequency control of interconnected power system using grey wolf optimization', *Swarm Evol. Comput.*, 2016, **27**, pp. 97–115

[11] Sahu, R.K., Panda, S., Rout, U.K., *et al.*: 'Teaching learning based optimization algorithm for automatic generation control of power system using 2-DOF PID controller', *Int. J. Elect. Power Energy Syst.*, 2016, **77**, pp. 287–301

[12] Irsheid, A.M.: 'Load frequency control and automatic generation control using fractional-order controllers', *Electr. Eng.*, 2010, **91**, pp. 357–368

[13] Patra, S., Sen, S., Ray, G.: 'Design of robust load frequency controller: H_∞ loop shaping approach', *Electr. Power Compon. Syst.*, 2007, **35**, (7), pp. 769–783

[14] Saxsena, S., Hote, Y.V.: 'Load frequency control in power system via internal model control scheme and model order reduction', *IEEE Trans. Power Syst.*, 2013, **28**, (3), pp. 2749–2757

[15] Mohanty, B.: 'TLBO optimized sliding mode controller for multi-area multi-source nonlinear interconnected AGC system', *Int. J. Elect. Power Energy Syst.*, 2015, **73**, pp. 872–881

[16] Bevranic, H., Yasunori, M., Kiichiro, T.: 'Sequential design of decentralized load frequency controller using μ-synthesis and analysis', *Energy Convers. Manag.*, 2004, **46**, (4), pp. 865–881

[17] Abd-Elazim, S.M., Ali, E.S.: 'Load frequency controller design via BAT algorithm for nonlinear interconnected power system', *Int. J. Elect. Power Energy Syst.*, 2016, **77**, pp. 166–177

[18] Raju, M., Saikia, L.C., Sinha, N.: 'Automatic generation control of a multi-area system using ant lion optimizer algorithm based PID plus second order derivative controller', *Int. J. Elect. Power Energy Syst.*, 2016, **80**, pp. 52–63

[19] Abdelaziz, A.Y., Ali, E.S.: 'Cuckoo search algorithm based load frequency controller design for nonlinear interconnected power system', *Int. J. Elect. Power Energy Syst.*, 2015, **73**, pp. 632–643

[20] Mohanty, B., Panda, S., Hota, P.K.: 'Controller parameters tuning of differential evolution algorithm and its application to load frequency control of multi-source power system', *Int. J. Elect. Power Energy Syst.*, 2014, **54**, pp. 77–85

[21] Daneshfar, F., Bevrani, H.: 'Multiobjective design of load frequency control using genetic algorithms', *Elect. Power Energy Syst.*, 2012, **42**, pp. 257–263

[22] Farhangi, R., Boroushaki, M., Hosseini, S.H.: 'Load–frequency control of interconnected power system using emotional learning-based intelligent controller', *Int. J. Elect. Power Energy Syst.*, 2012, **36**, pp. 76–83

[23] Guha, D., Roy, P.K., Banerjee, S.: 'Application of backtracking search algorithm in load frequency control of multi-area interconnected power system', *Ain Shams Eng. J.*, 2016 (in press)

[24] Pothiya, S., Ngamroo, I., Runggeratigul, S., *et al.*: 'Design of optimal fuzzy logic based PI controller using multiple Tabu search algorithm for load frequency control', *Int. J. Control Autom. Syst.*, 2006, **4**, (2), pp. 155–164

[25] Guha, D., Roy, P.K., Banerjee, S.: 'Application of modified biogeography based optimization in AGC of an interconnected multi-unit multi-source AC-DC linked power system', *Int. J. Energy Opt. Eng.*, 2016, **5**, (3), pp. 1–18

[26] Shankar, G., Mukherjee, V.: 'Load frequency control of an autonomous hybrid power system by quasi-oppositional harmony search algorithm', *Int. J. Elect. Power Energy Syst.*, 2016, **78**, pp. 715–734

[27] Shiva, C.K., Mukherjee, V.: 'A novel quasi-oppositional harmony search algorithm for AGC optimization of three-area multi-unit power system after deregulation', *Int. J. Eng. Sci. Tech.*, 2016, **19**, pp. 395–420

[28] Shiva, C.K., Mukherjee, V.: 'A novel quasi-oppositional harmony search algorithm for automatic generation control of power system', *Appl. Soft Comput.*, 2015, **35**, pp. 749–765

[29] Sahu, R.K., Panda, S., Pradhan, P.C.: 'Design and analysis of hybrid firefly algorithm-pattern search based fuzzy PID controller for LFC of multi area power systems', *Int. J. Elect. Power Energy Syst.*, 2015, **69**, pp. 200–212

[30] Panda, S., Mohanty, B., Hota, P.K.: 'Hybrid BFOA–PSO algorithm for automatic generation control of linear and nonlinear interconnected power systems', *Appl. Soft Comput.*, 2013, **13**, pp. 4718–4730

[31] Alam, S., Singh, A., Guha, D.: 'Optimal solutions of load frequency control problem using oppositional krill herd algorithm'. IEEE First Int. Conf. on Control, Measurement and Instrumentation (CMI), Jadavpur University, India, 2016, pp. 6–10

[32] Guha, D., Roy, P.K., Banerjee, S.: 'Application of krill herd algorithm for optimum design of load frequency controller for multi-area power system network with generation rate constraint'. Proc. fourth Int. Conf. on Frontiers in Intelligent Computing: Theory and Applications (FICTA) 2015, Advances in Intelligent Systems and Computing, 2015, vol. **404**, pp. 245–257

[33] Mirjalili, S.: 'Moth-flame optimization algorithm: a novel nature-inspired heuristic paradigm', *Knowledge-Based Syst.*, 2015, **89**, pp. 228–249

[34] Mirjalili, S.: 'Dragonfly algorithm: a new meta-heuristic optimization technique for solving single-objective, discrete, and multi-objective problems', *Neural Comput. Appl.*, 2016, **27**, (4), pp. 1053–1073

[35] Civicioglu, P.: 'Transforming geocentric Cartesian coordinates to geodetic coordinates by using differential search algorithm', *Comput. Geosci.*, 2012, **46**, pp. 229–247

[36] Rao, R.V.: 'Jaya: a simple and new optimization algorithm for solving constrained and unconstrained optimization problems', *Int. J. Ind. Eng. Comput.*, 2016, **7**, pp. 1–16

[37] Mirjalili, S., Mirjalili, S.M., Hatamlou, A.: 'Multi-verse optimizer: a nature-inspired algorithm for global optimization', *Neural Comput. Appl.*, 2016, **27**, (2), pp. 495–513

8 Appendx

Nominal values of test system-1 [6]

Parameters of investigated test system-1 are as follows:

$P_{ri} = 2000\,\text{MW}$, $f = 50\,\text{Hz}$, $T_{gi} = 0.08\,\text{s}$, $T_{ti} = 0.3\,\text{s}$, $T_{ri} = 10\,\text{s}$, $K_{ri} = 0.5$, $R_i = 2.4\,\text{Hz/p.u. MW}$, $B_i = 0.425\,\text{p.u. MW/Hz}$, $T_{ps} = 20\,\text{s}$, $K_{ps} = 120\,\text{Hz/p.u.}$, $2\pi T_{i,j} = 0.545$, $K_\text{P} = 1$, $K_\text{I} = 5$, $K_\text{D} = 4$, $T_w = 1$, $a_{12} = 1$.

Nominal values of test system-2 [4]

Parameters of investigated test system-2 are as follows:

$f = 60\,\text{Hz}$, $T_{gi} = 0.08\,\text{s}$, $T_{ti} = 0.3\,\text{s}$, $T_{ri} = 10\,\text{s}$, $K_{ri} = 0.5$, $R_i = 2.4\,\text{Hz/p.u. MW}$, $B_i = 0.425\,\text{p.u. MW/Hz}$, $T_{ps} = 20\,\text{s}$, $K_{ps} = 120\,\text{Hz/p.u.}$, $T_{ij} = 0.544$.